

Gyrokinetic Simulation of Tokamak Fusion Plasmas

Principal Investigator: Scott E. Parker

*Department of Physics
Renewable and Sustainable Energy Institute
University of Colorado, Boulder*

Introduction/Overview

This is an application to the U.S. DOE, Office of Fusion Energy Sciences Financial Assistance Funding Opportunity Announcement “Theoretical Research in Magnetic Fusion Energy Science” Number DE-FOA-0002226. This grant supports the ongoing theoretical fusion plasma program at the University of Colorado investigating gyrokinetic turbulence and transport. This proposal is a renewal of grant DE-FG02-08ER54954. This research grant funds a postdoctoral scholar (Dr. Haotian Chen) half time, a graduate research assistant (Stefan Tirkas, Physics Ph.D. graduate student), one-month of Scott Parker’s summer salary, and other related expenses, including travel and computer software and supplies. We also typically support an hourly undergraduate physics student doing research (Matthew Mitchell). Besides fulfilling the education mission, undergraduate students can be quite productive (see “Fourier-basis particle simulation” below) and are relatively inexpensive to support. This funding is critical for our group’s operation. Currently, our research group also receives funding from the SciDAC program in edge physics and the DOE Exascale Computing Project for core-edge coupling of gyrokinetic codes. This proposal targets turbulent transport in tokamak plasmas, enables student mentoring, and takes advantage of synergies between other funded projects. We will work in two areas: 1) underlying physics of electron scale turbulence, and 2) inward pinch of cold impurity ions. We will use both the GEM gyrokinetic particle and GENE continuum simulation codes in our investigations. We plan to continue to fully support, maintain, and further develop GEM, while also initiating research utilizing GENE, where it is advantageous to do so.

Electron scale turbulence, driven by the electron temperature gradient (ETG) instability, can be highly anisotropic because zonal flow generation is impeded by the adiabatic response of the ions [Dorland00, Jenko00]. This anisotropy manifests as visible “streamers” and results in gyrokinetic simulations producing experimentally significant electron energy transport in certain parameter regimes (e.g., moderate magnetic shear, low $\alpha = [q^2/R]d\beta/dr$) even though ETG occurs at electron scales. More recent large-scale GYRO simulations covering both ion and electron scales (so-call “multiscale”), show streamers persist in C-MOD L-mode parameter regimes near marginal to the ion temperature gradient (ITG) instability [Howard15, Howard16]. The importance of the electron scale and the existence of ETG streamers was found for DIII-D (H-mode) ITER baseline case as well [Holland17]. The persistence of ETG streamers in multiscale turbulence has been studied extensively [Jenko04, Holland04, Maeyama15, Goerler08].

Isotropization due to the ExB nonlinearity is robust in magnetized plasmas and generally seen in fluid models [Hasegawa78a, Terry83, Wakatani83]. In these simple fluid models, the polarization nonlinearity has a cross-product $\mathbf{k}_1 \times \mathbf{k}_2$, $\mathbf{k} = \mathbf{k}_1 \times \mathbf{k}_2$, resulting in rotation in k-space [Hasegawa78b]. It is somewhat

puzzling that ETG streamers persist in the saturated turbulent state. One simple argument for the persistence of the streamers is the fact that k_x is nearly zero and there can be no rotation in $k_x k_y$ -space, where x and y as the two field-line following coordinates perpendicular to B . However, with turbulent fluctuations, one might expect fluctuations at finite- k_x to allow for isotropization. This mechanism will be discussed further in the “Proposed Work and Project Objectives” section below. It is important to realize that the gyrokinetic simulations are toroidal and that insight from slab turbulence models may be limited. Global toroidal GTC simulations show the persistence of the linear eigenmode structure, but find low flux levels due to the low nonlinear saturation level [Lin05]. These results were supported by toroidal gyrokinetic mode-coupling theory [LChen05], but there were some concerns raised regarding discrete particle noise [Nevins05]. Additionally, the global simulations reported were for quite small tokamak plasmas (a tokamak minor radius of only 500 electron gyro-radii) [Lin07].

We plan to investigate the nonlinear isotropization, or the lack of it, in the context of the various nonlinear saturation mechanisms using both toroidal gyrokinetic theory and simulation. Saturation mechanisms include quasi-linear flattening [Idomura05], secondary Kelvin-Helmholtz-type instabilities [Jenko04], either by parallel [Cowley91] or perpendicular [Dorland00] flows, or toroidal mode coupling [LChen05]. Additionally, there can be a long-time buildup (proportional to time) of zonal flows via the Hinton-Rosenbluth random-walk mechanism [Rosenbluth98, Hinton99, Parker06, Colyer17] where the zonal flow is excited from turbulent background fluctuations. A zonal flow buildup proportional to time is a fairly clear signature of the random-kick mechanism. However, it is unclear if the more recent simulation results [Colyer17, Holland17] showing fine-scale zonal flow generation are from the random-kick mechanism or a modulational instability of the zonal flow. We propose to use nonlinear toroidal gyrokinetic theory to study how the linear ETG eigenmodes can act as a pump wave for driving the zonal flow unstable via a modulational instability. We plan to study under what parameter regimes (e.g., temperature gradient and magnetic shear) such a parametric instability produces a spontaneous generation of zonal flow. Though gyrokinetic simulations indicate ETG transport is primarily electrostatic, we will investigate electromagnetic effects with increasing plasma β , including magnetic field line flutter and zonal field generation [Hoang98, Holland02, Srivastav19].

We are currently running both GENE [Jenko00, Goerler11] and GEM for the ETG turbulence problem. Additionally, we have a simple (a toy model) Hasegawa-Mima-type fluid simulation for ETG, as well as linear and nonlinear toroidal gyrokinetic theory. We will compare and contrast these multiple levels of theory and simulation to improve our understanding of the nonlinear saturated state. Our ultimate objective is to develop a theory that determines under what tokamak plasma parameter regimes do the highly anisotropic ($k_x \ll k_y$) ETG streamers persist and cause significant electron heat transport. Finally, we will explore if there are any limitations to the ion gyrokinetic equations in the electron scale with $k_\perp \rho_e \sim 1$, $k_\perp \rho_i \gg 1$. We will do this using the full-kinetic (or Lorentz) ion model recently developed in GEM over the previous grant period.

A second problem we will investigate is the inward pinch of cold impurity ions in the edge pedestal. Impurity transport is a topical area due to the long-time buildup of impurities in the core, potentially leading to radiative power loss and termination of the discharge [Estrada05, Fulop06, Howard12, Esteve18]. Impurity and Helium ash buildup in a fusion reactor is also an important issue due to the dilution of the fuel DT species. In the EAST, long-pulse superconducting tokamak, impurities limit the length of performance discharges to tens of seconds [Wan17, Wang18]. Controlling the impurity buildup is a critical issue in long-

pulse experiments. More importantly, there is renewed interest in impurity transport due to the tungsten divertor design in ITER and related supporting experiments on JET, ASDEX-U, and DIII-D. The JET ITER-like wall experiments show the accumulation of tungsten (W) being a significant concern limiting performance [Angioni14]. W ($Z=74$), is not the only material of interest for plasma-facing components. Other materials such as molybdenum (Mo, $Z=42$) and low- Z Beryllium (Be, $Z=4$) have good plasma material boundary characteristics. Tungsten will not be fully ionized even in the core and will have multiple charge state species. Be is being used for the chamber wall for the JET ITER-like wall experiments. Additionally, other lower- Z impurities such as N ($Z=7$), Ne ($Z=10$), or Ar ($z=18$) are gas injected into the scrape-off layer to radiate power and reduce the heat flux to the divertor plate [Bonnin17].

Previously, we have shown that a cold ion component exhibits a strong inward pinch, which is a thermodynamically preferred mechanism [Wan10, Wan11]. Specifically, hot ions going outward and cold ions going inward reduces the free energy of a plasma discharge with a strong ion temperature gradient. A cold ion pinch may play a role in edge density pedestal transport [Wan11]. Additionally, cold tritium ions pinch inward, resulting in a possible fueling mechanism [Wan10]. We would like to extend this principle to other impurity ion species. Impurity neutrals penetrate the edge pedestal plasma and are colder than the background ions. These cold neutrals then ionize, through ionization and charge-exchange, where charge exchange is more dominant for hydrogen species and ionization dominant for other impurities [Wesson11]. The neutral penetration leads to a cold impurity ion component. Neutral transport and source physics are beyond the capability of the GEM and GENE codes. But, by using specified density and temperature profiles, we can investigate the associated anomalous pinch of the cold impurity ions due to microturbulence. GENE will also allow the investigation of the combination of neoclassical and turbulence effects, which are essential for a complete picture of impurity transport [Fulop06, Esteve18].

We will use neutral and ion profiles from SOLPS provided by J. Canik, ORNL, to help choose appropriate profiles for the cold impurity ion components. SOLPS modeling does not presently treat the cold ion components separately, but the neutral temperature is well below the bulk ion plasma temperature inside the separatrix [Wan11, Canik19]. We will use the neutral density and temperature to infer cold ion component densities and temperatures. GENE simulations with impurities and collisional effects will be done in the closed-flux-surface pedestal region, and we will model the cold component impurity ion species resulting from the cold edge neutral source analytically. We will also use fluid impurity transport theory for further understanding and guidance [Estrada05, Fulop06, Wan10, Wan11].

In contrast to lower- Z impurities, such as C, Ar, Ne, etc., which can be modeled well using gyrokinetics, tungsten (and other high- Z ions) has a relatively large mass and are not fully ionized, leading to a relatively small charge to mass ratio compared to the bulk ions. Therefore, high- Z ions can have a large gyroradius compared to associated equilibrium gradients. Full dynamics Z ions have been studied previously using a Monte-Carlo divertor transport code [Yamamoto17]. In addition to GENE simulations, we propose to model full-kinetic (Lorentz force) tungsten ions in GEM to investigate the large orbit effects of W in the context of edge pedestal transport. This work will utilize existing full-kinetic ion capability in GEM that was developed in the last funding cycle. The impurity pinch research problem will be discussed further in the “Proposed Research and Project Objectives” Section below.

Background and Previous Accomplishments

Description of the GEM code

The GEM code is a gyrokinetic delta-f Particle-In-Cell (PIC) code that was originally developed for the study of tokamak core micro-turbulence and anomalous transport. The details of the GEM code algorithms and numerical methods can be found in Refs. [Chen03, Chen07]. A User's Manual is available at the web site: www.gemgyrokinetic.org. GEM uses the field-aligned coordinates in general magnetic equilibria given by either the Miller equilibrium model [Miller98] or a numerically calculated equilibrium [Wan15]. The numerical magnetic equilibrium, such as output from EFIT, can be interfaced either directly, or by using Miller parameterization. Electromagnetic perturbations are included using the parallel canonical momentum formalism. GEM uses an explicit time advance and expands the electron distribution about an adiabatic response leading to an approximate timestep constraint of a $k_{\parallel}v_{te}\Delta t \sim 1$. A finite- β Ampere solver is used allowing accurate simulation of Alfvén waves or drift-wave type turbulence. GEM is radially global, with multiple ion species, arbitrary density and temperature profiles, electron-ion collisions, and a specified equilibrium E_r profile. For long-time simulation, a coarse-graining procedure has been developed to control the secular growth of the mean square of the particle weights, which is a numerical manifestation of collisionless phase-space filamentation.

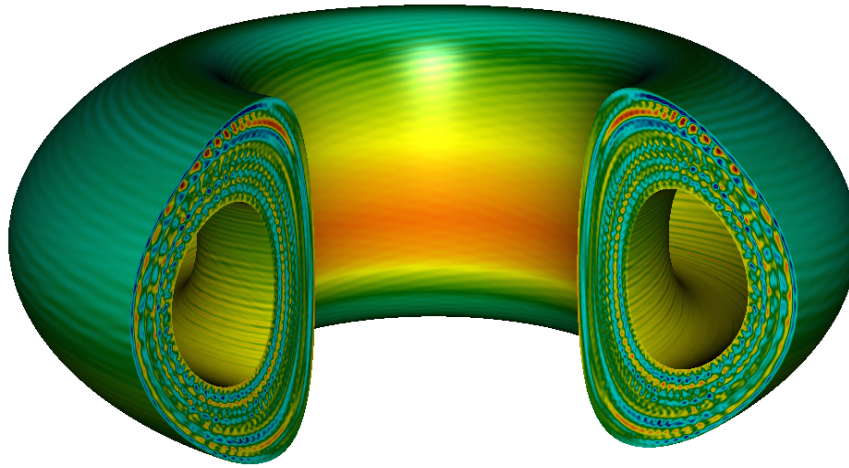


Figure 1: The GEM code. More unstable edge instabilities result in mode excitation and turbulence spreading across the plasma volume.

GEM's electromagnetic kinetic electron algorithm has been benchmarked with continuum codes GS2, GYRO, and GENE both linearly and nonlinearly [Nevins07, Ernst09, Wang12, Bravenec13]. It is the only particle code that has participated in Bravenec's gyrokinetic code verification project [Wang12, Bravenec13]. Additionally, GEM has routinely engaged in comparisons and benchmarking exercises with the U.S. particle codes GTC and XGC1 [Spong12, Chen13, Hager17].

Nonlinear GEM simulations of microtearing turbulence in NSTX

It is well known that microtearing can produce substantial electron heat flux in high beta machines in the presence of electron temperature gradients. Microtearing modes were first studied with gyrokinetic simulation in slab geometry [Sydora01, Wan05, Rodgers07, Numata11]. The GTS code has studied this problem as well [Startsev14]. For spherical tokamaks, it is observed that the microtearing mode can be the most-unstable mode in both the core [Applegate04, Applegate07, Wong07, Smith11, Guttenfelder11, Guttenfelder12a, Guttenfelder12b, Roach05] and edge [Canik13, Dickinson12, Dickinson13]. This is a plausible candidate to explain the collisional scaling of global confinement time observed in such machines. The microtearing mode (MTM) has been found to be important in conventional tokamaks [Kenser99, Told08, Doerk11, Doerk12, Moradi13, Saarela13, Manz14] as well as reverse field pinch machines [Predebon10, Predebon13]. For conventional tokamaks, the MTM can act as a precursor to the ELM [Manz14, Hillesheim16]. Additionally, linearly subdominant MTMs can contribute to electromagnetic ITG turbulence [Hatch13]. In H-mode pedestal simulations of the JET “ITER-like wall” case, the MTM is found to contribute to the total electron heat flux substantially [Hatch16].

Due to the potential importance of microtearing in both the core [Guttenfelder11] and edge [Canik13] of the National Spherical Torus Experiment (NSTX), we have been studying microtearing turbulence using NSTX equilibria and profiles with GEM [Chowdhury16, Chowdhury20]. Earlier parts of this work were presented as an invited talk by Dr. J Chowdhury at the *2016 Sherwood Fusion Theory Conference*. To our knowledge, this is the first such particle code study of microtearing using realistic experimental parameters. We have done a comprehensive linear study in both the edge and core regions [Chowdhury16], as well as nonlinear turbulence simulations [Chowdhury20]. We observe that the MTM in the core depends upon the electron-ion collisions. Still, in the edge region (near the pedestal top), the MTM exhibits very little dependence on collisions both linearly and nonlinearly. Fig. 2 shows that the nonlinear heat flux is insensitive to collisionality. The MTM exists even as the collision frequency approaches zero. This result is particularly interesting because earlier theoretical predictions require finite collisionality for the MTM to be unstable. This might be important for pedestals of higher temperatures in NSTX-U operation. We also observe that the effect of the electrostatic potential is significant, which is again in contrast to the earlier theories which drop the electrostatic potential altogether from calculations.

Nonlinear MTM simulations have been performed for the edge parameters similar to what one would find at the top of an NSTX H-mode pedestal [Chowdhury20]. These edge simulations require high resolution and are challenging to undertake. The electron heat flux from the MTM is mostly due to the electromagnetic component, and the ion heat flux is negligible compared to the electron heat flux. We also find that electron heat flux initially increases with the beta peaking at $\beta_e=0.013$, but then decreases with higher in beta [Chowdhury20]. The electron heat flux is somewhat insensitive to experimental levels (pedestal top) of ExB shear, as shown in Fig. 3.

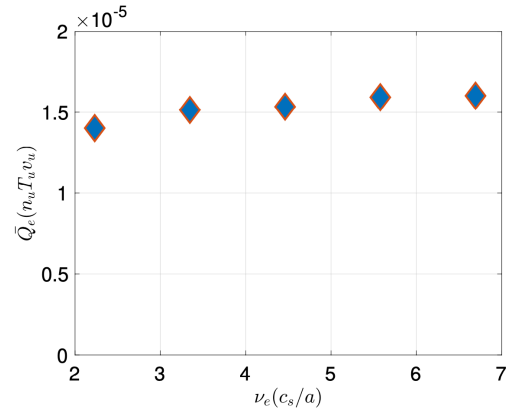


Figure 2: Electron heat flux for microtearing versus collisionality [Chowdhury20].

Saturation mechanisms of energetic particle driven Alfvén eigenmodes

GEM has been successful for studying Alfvén eigenmodes in tokamak plasmas excited by energetic particles, e.g., see Ref. [Chen18]. EP driven Alfvén waves are a central concern for future fusion reactors and have been studied extensively. The main goal of nonlinear EP simulation is to determine the mode amplitude and assess the EP loss or redistribution. This work is challenging due to the kinetic nature of EP physics. For near marginal instabilities, it can be shown that the wave-particle nonlinearity is significant [Berk96]. If this is the case, then it is possible to treat the Alfvén waves using a quasi-linear approximation with a fixed mode structure and frequency. Only the mode amplitude evolves in response to the EP wave-particle interaction. The thermal kinetic damping effects can be pre-computed with eigenmode analysis. However, as the wave amplitude increases, the thermal species nonlinearity can lead to the generation of zonal structures [LChen16, Todo10] and significantly change the nonlinear behavior.

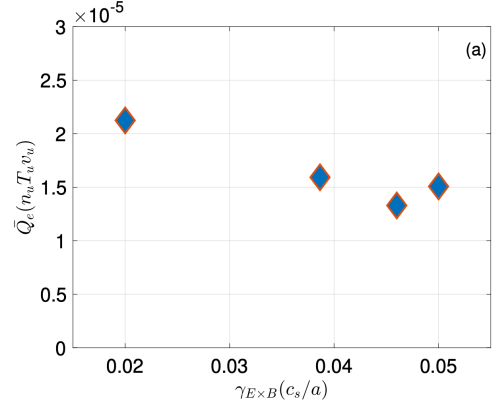


Figure 3: Microtearing electron heat flux versus shearing rate from [Chowdhury20].

In the previous funding cycle, we have studied the nonlinear evolution of reversed shear Alfvén eigenmodes (RSAE) using gyrokinetic ions and fluid electrons. When only the energetic particle nonlinear effects are included, the saturation amplitude of a single-n RSAE follows the trapping scaling, $\delta B/B \sim \gamma^2$. When the nonlinear effects of thermal ions and electrons are included, zonal structures are force generated but do not affect the saturation amplitude for $\gamma/\omega < 0.03$. No spontaneous generation of zonal is observed, in contrast to ITG turbulence. At larger energetic particle drive, the effects of zonal structures cause a significant reduction in the RSAE saturation amplitude, red circles in Fig. 4. The decrease is not caused by the zonal flow shearing of the RSAE, but by the force-generated $n=0$ component in the thermal ion distribution function and the electron density. These $n=0$ perturbations lead to the nonlinear evolution of the RSAE mode structure and enhance damping [Chen18].

We have also studied this same problem with kinetic electrons. Kinetic electron effects on the linear RSAE mode are expected to be small. However, if fine spatial and temporal scales arise due to nonlinear coupling, closure schemes used in the fluid models become questionable, and it is necessary to consider drift-kinetic electrons. At present, simulation of low-n electromagnetic modes with kinetic electrons is still challenging and requires novel discretization schemes for the electrons [Mishchenko14, Bao17]. Even with these difficulties, the direct

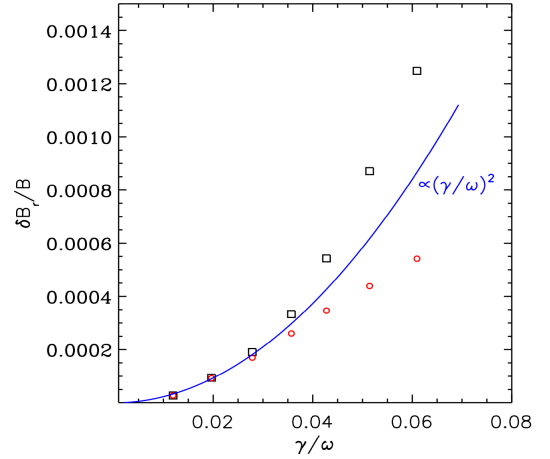


Figure 4: Peak root-mean-square value of the radial magnetic perturbation. Black squares show simulation with only the beam nonlinearity. Red circles show results with the thermal species.

GEM algorithm is still able to simulate low- n EP driven Alfvén modes. Linear benchmarking with the fluid electron model shows excellent agreement for the $n=3-6$ RSAEs. Nonlinear simulations with drift-kinetic electrons show zonal structures are excited by the thermal species due to self-coupling of the RSAE, with short radial scales. The nonlinearly generated fluctuations cause significant nonlinear damping of the RSAE. This effect is sensitive to the magnetic flutter term. As shown in Fig. 5, drift-kinetic electrons reduce the beam particle flux by 50% at a moderate RSAE amplitude of $\delta B/B < 10^{-3}$. In general, drift-kinetic electrons are important for modeling EP transport. This is the first time nonlinear drift-kinetic electron effects have been included in PIC simulation of low- n EP driven Alfvén modes. Future work will involve finalizing the nonlinear results with drift-kinetic electrons during the next funding cycle.

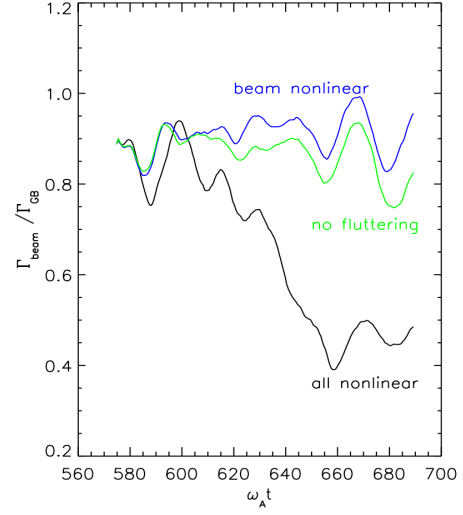


Figure 5: Nonlinear RSAE particle flux. Blue line is with fluid electrons. The green line includes kinetic electrons without magnetic flutter. Black line is the full-physics result.

Progress on full-kinetic ions in GEM

There is a long history of hybrid simulations using Lorentz ions and guiding center electrons for various applications [Tanaka93]. Lorentz ions/fluid electrons have been proposed for extended-MHD closure [Barnes08], and have been used extensively to study kinetic-MHD stability in reversed field configurations [Belova00]. A Lorentz ion, gyrokinetic electron simulation model, was first developed to study magnetic reconnection in space plasmas [YLin05]. More recently, Lorentz ions and drift kinetic electrons have been used to study RF heating [Kuley15]. Previously, we developed a first-order implicit delta- f Lorentz ion drift-kinetic electron model [Chen09], specifically to study low-frequency microturbulence in magnetic fusion plasmas. An implicit method was used to eliminate the constraint on the time step imposed by the fast-compressional wave. We developed a more accurate second-order implicit Lorentz ion hybrid model [Cheng13]. We demonstrated the power of this model on the following test problems: the nonlinear evolution of tearing mode driven islands, nonlinear saturation of ion Landau damping of ion acoustics waves, and the ITG instability [Schnack13]. The unique aspect of our work is the use of implicit multiscale techniques to model low-frequency physics with Lorentz ions.

A key challenge is to avoid noise and stability constraints imposed by the ion Bernstein and lower-hybrid waves when studying low-frequency drift-wave-type turbulence. We have developed an implicit orbit averaging and sub-cycling algorithm scheme to allow for multiscale treatment of ion dynamics [Sturdevant16]. This model was extended to global simulation [Sturdevant17], and good agreement with gyrokinetics was obtained for linear ITG, see Fig. 6. We have

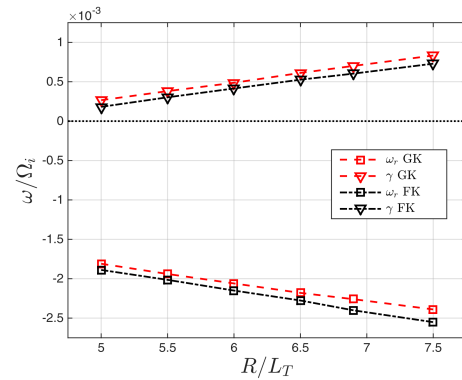


Figure 6: Global toroidal linear comparison between full kinetic and gyrokinetic in GEM [Sturdevant18].

made some progress simulating nonlinear ITG both in slab [Miecnikowski18] and toroidal [Hu18] geometries. Nonlinear slab results are shown in Fig. 7, where lower-hybrid oscillations are observed in the zonal flow modes. The ITG problem is an extreme test of full-kinetic simulation, yet very much in the comfort zone for gyrokinetic simulation. Hence, ITG provides an ideal testbed for developing competitive full-kinetic algorithms. We presented an invited talk at APS-DPP 2017, “Multiscale full kinetics as an alternative to gyrokinetics,” S. Parker.

Toroidal full-kinetic ion, gyrokinetic electron capability, is useful for verification of gyrokinetics in situations where gyrokinetic ordering may be marginal. However, low-frequency ion scale turbulence is difficult with GEM’s current implementation due to the small timestep and the large number of particles required for numerical stability. However, we can and will utilize this model for two important physics problems that are within the scope of the proposed work. We will study differences between gyrokinetic and full-kinetics for the ETG instability. Fig. 8 shows the effect of full-kinetic ions on ETG for Cyclone base case parameters using 32-point gyroaveraging for the gyrokinetic result. These results are preliminary and we do not see qualitative differences with full-kinetic ions. Continuing this work is part of the proposed work.

We will also examine the large orbits of Tungsten ions and other heavy impurities with $Z_e/m \ll e/m_i$, where m_i is the mass of the bulk ions and see the impact on large- Z impurity transport. For ETG turbulence, the gyrokinetic electron response dominates, and full-kinetic ions will function well, assuming electron-scale simulation domains. We will not attempt ion full-kinetic multiscale (ion scale domain size with electron scale grid resolution) simulations. For high- Z impurities, the impurity density is small, and the gyrokinetic bulk ion response dominates, allowing for well-behaved simulations.

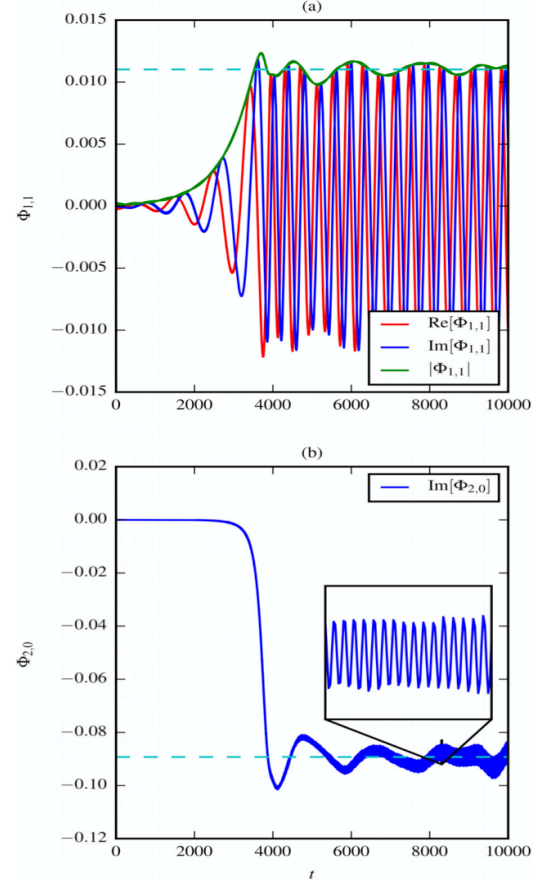


Figure 7: Full kinetic nonlinear saturation of the slab ITG instability (a) and zonal associate flow generation (b) [Miecnikowski18]. Lower-hybrid oscillations are observed in the zonal flow. Nonlinear saturation of a single toroidal mode is demonstrated in Ref. [Hu18].

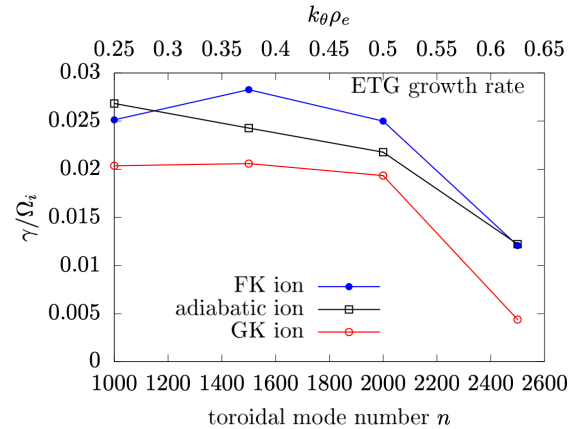


Figure 8: Comparison of linear growth rate for GEM simulations of the ETG mode with adiabatic electrons, gyrokinetic ions and full-kinetic ions.

Fourier-basis particle simulation

During the prior grant period, we developed a new grid-less particle simulation technique. It is well-known that particle simulations using a Fourier representation for the fields with no grid has excellent conservation properties relative to the particle-in-cell (PIC) method [Huang16, Evstatiev13]. However, such Fourier or grid-less simulations were inefficient because the deposition and particle field steps required summing over all Fourier modes. This resulted in $O(N_k N_p)$ time scaling, with N_k being the number of Fourier modes and N_p being the number of particles, while the conventional PIC method scales roughly as $O(N_p)$. We have improved upon this through the implementation of an unequally-spaced fast Fourier transform algorithm [Beylkin95, Dutt93], obtaining a time complexity equivalent to that of conventional PIC, but with much-improved accuracy and energy conservation. We recently published this result in the *Journal of Computational Physics* [Mitchell19]. The first author of this paper, Matthew Mitchell, is an undergraduate physics and computer science student working in our group. Mr. Mitchell will be a physics graduate student at Yale University in the fall of 2020.

We have recently developed a two-dimensional code with a relativistic, electromagnetic generalization of the Fourier-basis algorithm. The goal of this project is to develop an energy-conserving code with an efficient, non-dispersive Maxwell solver, with a focus on reducing or eliminating the numerical Cherenkov instability, which results from a nonphysical coupling between plasma oscillations and light waves [Godfrey74]. Spectral methods have previously been used to address the numerical Cherenkov instability [Yu15]. Using unequally spaced FFTs permits the Fourier components of the fields to be calculated directly from the particle positions without any aliasing. While this new particle simulation method was developed within the magnetic fusion energy sciences program, we expect that this algorithm will impact on other fields such as plasma wakefield acceleration.

Proposed Research and Project Objectives

In this section, we present our proposed research and identify the key project objectives. We plan research in two areas: 1) isotropization of electron-scale turbulence, and 2) pinch of cold impurities in the edge pedestal region.

Isotropization of electron-scale turbulence

We begin by discussing our proposed research on studying saturated ETG turbulence, to be able to theoretically predict for what tokamak plasma conditions, the associated electron heat transport is experimentally significant. At first brush, this might appear to be an old problem with seminal gyrokinetic simulations done 20 years ago [Dorland00, Jenko00]. However, the nonlinear behavior of streamers and associated fine-scale zonal flow generation continues to be quite topical [Colyer17, Holland17]. It still is not well understood under what conditions streamers persist, thereby producing significant electron energy transport. This is a fundamental problem for understanding the parameter dependence of electron temperature profiles in both core and edge tokamak plasmas. Case-by-case multiscale simulations are required to make connections with experiment due to the inherent nonlinearity of the streamer dynamics [Howard16, Holland17]. These individual multiscale simulations require extreme computational resources. Our research group has initiated running the GENE code in collaboration with G. Merlo and F. Jenko. See the attached Letters of Collaboration in Appendix 7.I. of the proposal. We have successfully reproduced the Goerler benchmark [Goerler14] with kinetic ions and electrons, see Fig. 9. There is sensitivity in this benchmark at around $k_y \rho_i = 0.65$, where there is a switch between the ITG and TEM branch. We have successfully run nonlinear ion and electron scale simulations with GENE as well.

GEM is well-benchmarked with GENE and other codes for the Goerler case [Hager17] and for many other cases, as discussed in the “Background and Previous Work” section above. We show the GENE Goerler case just to get familiar with running the GENE code and demonstrate GENE capability within the Colorado research group (results from physics Ph.D. graduate student Stefan Tirkas). We are not attempting multiscale simulations at this time due to the large amount of computing resources that would be required. We have run nonlinear ETG turbulence using both GEM and GENE. Fig.

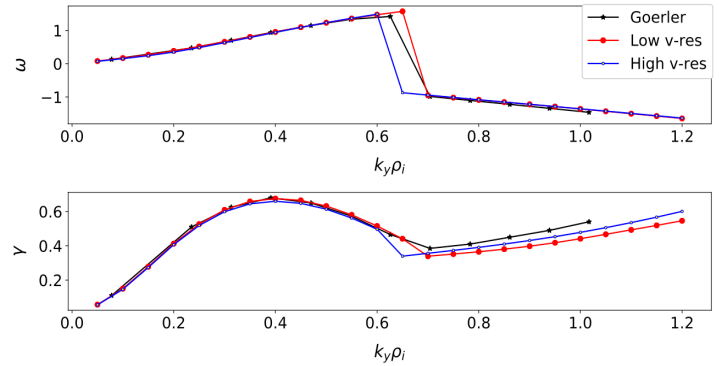


Figure 9: Goerler benchmark [Goerler14] using GENE. Demonstrating GENE simulation capability.

10 shows the linear growth rate for the ETG instability for the Goerler case ($T_i = T_e$) except with the ion temperature gradient set to zero benchmarking GEM and GENE. Nonlinear saturated streamers are shown in the electrostatic potential contour plot in Fig. 11 for the same parameters, as shown in Fig. 10.

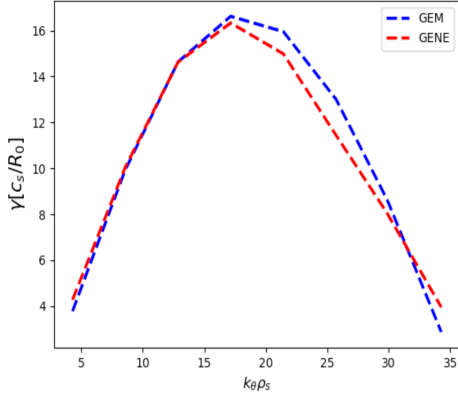


Figure 10: Linear benchmark between GENE and GEM with kinetic electrons and electrons.

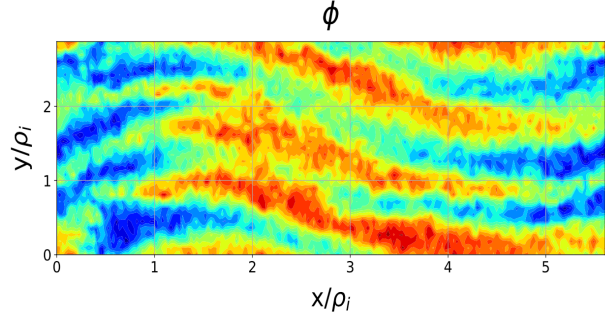


Figure 11: Nonlinear saturated streamers from running GENE for the same parameters as Fig. 10.

To illustrate the isotropization mechanism in conventional drift-wave turbulence without zonal flows, we have derived a simple Hasegawa-Mima-type ETG one-field fluid model using ion scale units with $\tau = T_e/T_i$

$$-(1 - \frac{1 + \tau}{2} \frac{m_e}{m_i} \nabla_{\perp}^2) \partial_t \Phi + \frac{1 + \tau}{2} \frac{r_n^2}{\rho_i^2} \frac{m_i}{m_e} \partial_t^{-1} \nabla_{\parallel}^2 \Phi + \frac{\tau(1 + \tau)(1 + \eta_e)m_e}{4m_i} \partial_y \nabla_{\perp}^2 \Phi + \frac{1 + \eta_e}{2} \partial_y \Phi + \frac{m_e(1 + \tau)^2}{m_i} \frac{r_n}{4\rho_i} [\hat{b} \times \nabla_{\perp} \Phi \cdot \nabla_{\perp}] \nabla_{\perp}^2 \Phi = 0.$$

We solve this equation pseudo-spectrally in the two-dimensions perpendicular to \mathbf{B} by setting $k_{\parallel} = 0$. We initialize the system with streamers along with small high- k fluctuations, as shown in the top panels of Fig. 12. The polarization nonlinearity (the last term on the left) isotropizes the turbulence, as shown in the bottom two panels of Fig. 12.

We plan to develop a gyrokinetic toroidal mode-coupling theory similar to Ref. [LChen05] but include the two-dimensional eigenmode structure. The equations are highlighted in Appendix 7.II., “Brief description of toroidal gyrokinetic theory for ETG turbulence” developed by postdoctoral scholar Dr. Haotian Chen. Appendix 7.II. is only a sketch of our theoretical framework, and further development of the theory is a key objective of the project. We can show the zonal flow modes are unstable to a modulational instability where the unstable ETG mode plays the role of a “pump wave” at sufficient pump wave amplitude. This spontaneous zonal flow generation mechanism, which depends on the amplitude of the pump, is shown in Fig. 13 using GENE. We plan to better understand under what conditions, or parameters (e.g., magnetic shear, gradients, safety factor), fine-scale zonal flow is generated at significant levels. We will compare to simulation results from GENE and GEM. We also will investigate at what amplitude does the $\mathbf{E} \times \mathbf{B}$ nonlinearity compete with linear toroidal mode coupling producing the radially elongated ballooning mode structure [Similon84]. Finally, using both toroidal gyrokinetic theory and simulation, we will study the long-time buildup of fine-scale zonal flow [Parker06, Colyer17]. The advantage of the toroidal gyrokinetic

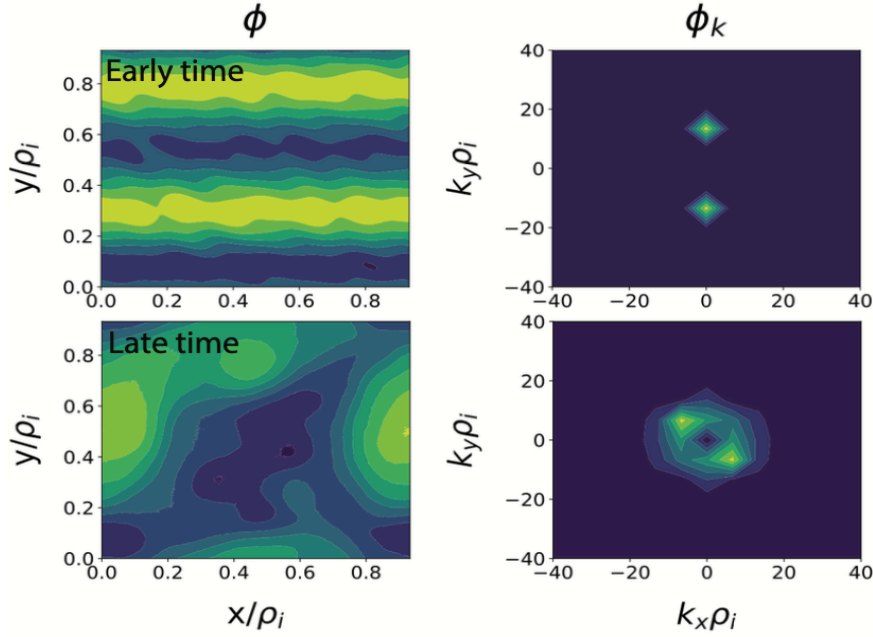


Figure 12: Simple ETG fluid model showing streamers lead to isotropic turbulence. Top panels show the streamer initial condition. Bottom panels show the later time stationary state.

theory, hand-in-hand with simulation, is that it allows better functional parameterization of the persistence of ETG anisotropy, which is an indicator of significant electron heat transport.

A related research problem we intend to explore is the effect of full-kinetic (Lorentz) ions. Last project period, we developed full-kinetic ion capability in GEM, and we plan to use this capability to investigate the adiabatic ion and gyrokinetic ion approximation for electron-scale turbulence. In toroidal gyrokinetic simulations, gyrokinetic ion capability for electron scale simulations is routine. Multiscale simulations demonstrate the importance of keeping ion scale instabilities. However, for the electron scale, $k_{\perp} \rho_e \sim 1$, $k_{\perp} \rho_i \gg 1$, and the conventional $k_{\perp} \rho_i \sim 1$ gyrokinetic ordering is violated for the ions. As shown in Fig. 8 above, we have done some linear tests for the ETG instability and find higher growth rates with full-kinetic ions. However, no qualitative differences are observed at this time. We plan to complete this work and include nonlinear results in the following grant period.

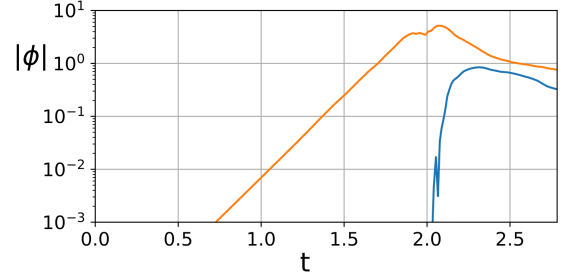


Figure 13: GENE simulation with one toroidal mode (blue) plus zonal flow mode (red) showing spontaneous generation of zonal flow. Arbitrary simulation units.

Pinch of cold edge impurities

As discussed above in the “Introduction/Overview” section, we propose to study the transport and inward pinch of impurity ions in the pedestal region. As shown in Fig. 14, the neutrals are colder than the bulk ions in the pedestal region [Wan11, Canik19]. Similar results have been obtained with SOLPS [Canik19]. This is due to neutral penetration in the edge [Langer82]. We plan to use SOLPS to obtain neutral species

profiles and bulk plasma profiles (from a fluid approximation). We will infer the cold-component impurity plasma analytically using ionization and charge exchange cross-sections, assuming Maxwellian bulk ion and electron plasma profiles from SOLPS. We will investigate a range of impurities, including tungsten and lower-Z species used for impurity seeding. Tungsten and other high-Z materials are especially challenging to model due to being only partially ionized and in multiple charge states.

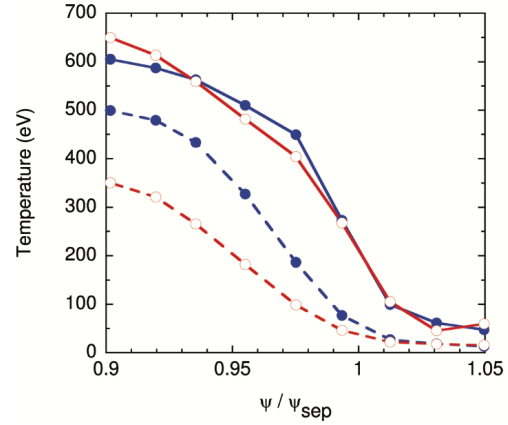


Figure 14: Bulk ion temperature (solid lines) and neutral temperature (dashed lines) for two low density DIII-D H-mode discharges using XGC0-DAGAS 2 [Wan11].

Our research will include investigating the importance of the charge-to-mass ratio of the impurity species for the anomalous pinch mechanism. One expects charge-to-mass ratios similar to the bulk ions will be pinched more effectively, but this needs to be explored further and is part of the proposed work. There are interesting results on JET where impurity seeding improves confinement, possibly by reducing impurities inside the separatrix [Belo04]. This behavior has not yet been investigated with the gyrokinetic turbulence codes. We plan to use the GENE code to do closed-field-line flux-tube and global simulations, including collisionality. GENE has the capability to model neoclassical effects. Collisionality is especially crucial for high-Z impurities, where it is enhanced due to charge ($Z > 1$). Getting a handle on how much turbulence (versus neoclassical effects) contributes to impurity transport is important [Fulop06, Esteve18]. Our GENE modeling will neglect the scrape-off layer and take the pedestal species profiles as given.

Finally, we plan to use fully-kinetic ion capability developed in GEM and discussed in the “Background and Previous Accomplishments” section above. Tungsten’s large mass ($A_w=184$) along with a typical charge state ($Z_w=40$) [Esteve18] may lead to finite-orbit effects being important [Yamoto17]. Numerically, GEM with full-kinetic ions should perform well because the impurity ion density will be small compared to the bulk plasma, and the impurity contribution will be perturbative. We can model the full-kinetic high-Z impurities two ways, either as tracer particles, or self-consistently, contributing to the charge density and current. As noted in Ref. [Yamoto17], the gyroradius of the tungsten ions can be comparable to equilibrium gradient scale lengths, and finite orbit transport can become important.

Timetable with Itemized Tasks

Here we list itemized tasks categorized by the year of the project and briefly summarize the work scope in bullet format.

Year 1

- Initialize the ETG fluid simulation with the saturated fluctuations coming from the GENE code to see the extent of turbulence isotropization.
- Develop a toroidal gyrokinetic theory of the modulational instability zonal flow mechanism for ETG. Determine under what conditions, e.g. low magnetic shear, mode amplitude, the zonal flow will be generated.
- Run GENE simulations with one eigenmode (high- n) and zonal flow ($n=0$) to compare with the theory in the bullet above.
- Parameterize density and temperature impurity neutral profiles for Carbon and other lower- Z impurity seeding neutrals (N, Ne, Ar). Data provided by SOLPS, in collaboration with J. Canik, ORNL.
- For given neutral density and temperature profiles, develop a simple model to infer the corresponding cold-component ion impurity species temperature and density profiles based on ionization and charge-exchange cross-sections.
- Begin preliminary GENE runs showing the cold impurity pinch mechanism.

Year 2

- Use GENE and GEM simulations, along with nonlinear gyrokinetic theory, to predict under what conditions ETG streamers persist.
- Nonlinear GENE parameter scans to investigate ETG spectral properties to test theoretical predictions.
- Submit a manuscript on the parameter dependence of ETG spectral properties (anisotropic vs. isotropic) and zonal flow properties.
- Benchmark GEM and GENE linearly and nonlinearly for edge H-mode DIII-D ETG cases. New work for GEM includes running in the $k_{\perp}\rho_i \gg 1$ limit with a 16 or 32-point particle gyroaverage.
- Parameterize density and temperature impurity profiles for multiple charge state high- Z Tungsten. The neutral profile data will be obtained from SOLPS.
- Investigate the turbulent impurity pinch effect for Carbon and low- Z impurities.

Year 3

- Apply full-kinetic ion capability in GEM to ETG turbulence and compare with well-resolved (16 or 32-point particle gyroaverage) the gyrokinetic ions.
- Study the accuracy of gyrokinetic equations for electron scale turbulence in H-mode edge pedestal plasmas using full-kinetic ions in GEM.
- Continue studying the parameter dependence of steamer persistence using GENE and gyrokinetic theory and investigate implications for H-mode edge pedestal on DIII-D and NSTX-U.

- Investigate the impurity pinch effect for multiple charge states of tungsten. See how strong the effect is relative to lower-Z species.
- Utilize full-kinetic capability in GEM to investigate the effects of large Tungsten orbits on edge transport.
- Submit a manuscript on turbulence-driven impurity transport in H-mode edge pedestal plasmas.

References Cited

- [Angioni14] C. Angioni, et al., Nucl. Fusion **54** 083028 (2014)
- [Applegate04] D. Applegate, et al., Phys. Plasmas **11** 5085 (2004)
- [Applegate07] D. Applegate, et al., Plasma Phys. Controlled Fusion **49** 1113 (2007)
- [Bao17] J. Bao, D. Liu, and Z. Lin, Phys. Plasmas **24** 102516 (2017)
- [Belo04] P. Belo, et al., Plasma Phys. Control. Fusion **46** 1299 (2004)
- [Barnes2008] D. Barnes, J. Cheng and S. Parker, Phys. Plasmas **15** 055702 (2008)
- [Belova2000] E. Belova, et al., Phys. Plasmas **7** 4996 (2000)
- [Bravenec13] R. Bravenec, et al., Phys. Plasmas **20** 104506 (2013)
- [Berk96] H. Berk, et al, Phys. Plasmas **3** 1827 (1996)
- [Beylkin95] G. Beylkin, Appl. Comput. Harmonic Anal. **2** 363 (1995)
- [Bonnin17] X. Bonnin, et al., Nucl. Mat. Energy **12** 1100 (2017)
- [Canik13] J. Canik, et al., Nucl. Fusion **53** 113016 (2013)
- [Canik19] private communication (2019)
- [LChen05] L. Chen, F. Zonca, Z. Lin, Plasma Phys. Control. Fusion **47** B71 (2005)
- [LChen16] L. Chen and F. Zonca, Rev. Mod. Phys. **88** 015008 (2016)
- [Chen03] Y. Chen and S. Parker, J. Comput. Phys. **189** 463 (2003)
- [Chen07] Y. Chen and S. E. Parker, J. of Comput. Phys. **220** 839 (2007)
- [Chen13] Y. Chen, et al., Phys. Plasmas **20** 012109 (2013)
- [Chen09] Y. Chen and S. Parker, Physics of Plasmas **16** 052305 (2009)
- [Chen18] Y. Chen, et al., Phys. Plasmas **25** 032304 (2018)
- [Cheng13] J. Cheng, S. Parker, Y. Chen, D. Uzdensky, J. Comput. Phys. **20** 364 (2013)
- [Chowdhury16] J. Chowdhury, et al., Phys. Plasmas **23** 012513 (2016)
- [Chowdhury20] J. Chowdhury, Y. Chen, S. Parker, Phys. Plasmas **27** 042309 (2020)
- [Colyer17] G. J. Colyer et al., Plasma Phys. Control. Fusion **59** 055002 (2017)
- [Cowley91] S.C. Cowley, R.M. Kulsrud, R. Sudan, Phys. Plasmas **3** 2767 (1991)
- [Dickinson12] D. Dickinson, et al., Phys. Rev. Lett. **108** 135002 (2012)
- [Dickinson13] D. Dickinson, et al., Plasma Phys. Controlled Fusion **55** 074006 (2013)
- [Doerk11] H. Doerk, et al., Phys. Rev. Lett. **106** 155003 (2011)
- [Doerk12] H. Doerk, et al., Phys. Plasmas **19** 055907 (2012)
- [Dorland00] W. Dorland, et al., Phys. Rev. Lett. **85** 5579 (2000)
- [Dutt93] A. Dutt, V. Rokhlin, SIAM J Sci. Comput. **14** 1368 (1993)
- [Ernst09] D. Ernst, et al., Phys. Plasmas **16** 055906 (2009)
- [Estrada05] C. Estrada-Mila, J. Candy, R. Waltz, Phys. Plasmas **12** 022305 (2005)
- [Esteve18] D. Esteve, et al., Nucl. Fusion **58** 036013 (2014)
- [Fulop06] T. Fulop, J. Weiland, Phys. Plasmas **13** 112504 (2006)
- [Evstatiev13] G. Evstatiev and B. A. Shadwick, J. Comput. Phys. **245** 376 (2013)
- [Godfrey74] B. B. Godfrey, J. Comput. Phys. **15** 504 (1974)
- [Goerler08] T. Goerler, F. Jenko, Phys. Rev. Lett. **100** 185002 (2008)
- [Goerler11] T. Goerler et al., J. Comput. Phys. **230**, 7053 (2011)
- [Goerler14] T. Goerler, et al., Phys. Plasmas **21** 122307 (2014)
- [Guttenfelder11] W. Guttenfelder, et al., Phys. Rev. Lett. **106** 155004 (2011)
- [Guttenfelder12a] W. Guttenfelder, et al., Phys. Plasmas **19** 056119 (2012)
- [Guttenfelder12b] W. Guttenfelder, et al., Phys. Plasmas **19** 022506 (2012)
- [Hager17] R. Hager, et al., Phys. Plasmas **24** 054508 (2017)
- [Hasegawa78a] A. Hasegawa, Y. Kodama, Phys. Rev. Lett. **20** 1470 (1978)
- [Hasegawa78b] A. Hasegawa, K. Mima, Phys. Fluids **21** 87 (1978)
- [Hatch13] D. R. Hatch, et al., Phys. Plasmas **20** 012307 (2013)

[Hatch16] D.R. Hatch, et al., Nucl. Fusion **56** 104003 (2016)

[Hillesheim16] J. Hillesheim, et al., Plasma Phys. Controlled Fusion **58** 014020 (2016)

[Hinton99] F. Hinton, and M. Rosenbluth, Plasma Phys. Contr. Fusion **41** A653 (1999)

[Holland02] C. Holland, P.H. Diamond, Phys. Plasmas **9** 3857 (2002)

[Holland04] C. Holland, P.H. Diamond, Phys. Plasmas **11** 1043 (2004)

[Holland17] C. Holland et al., Nucl. Fusion **57** 066043 (2017)

[Howard12] N.T. Howard, et al., Nucl. Fusion **52** 063002 (2012)

[Howard15] N. Howard et al., Plasma Phys. Control. Fusion **57** 065009 (2015)

[Howard16] N. Howard et al., Nucl. Fusion **56** 014004 (2016)

[Hoang98] G.T. Hoang, et al., Nuc. Fusion **38** 117 (1998)

[Hu18] Y. Hu, M. Miecniowski, Y. Chen, S. Parker, MPDI Plasma **1** 105 (2018)

[Huang16] C.K. Huang, et al., Comput. Phys. Comm. **207** 123 (2016)

[Hoang98] G.T. Hoang, et al., Nuc. Fusion **38** 117 (1998)

[Hu18] Y. Hu, M. Miecniowski, Y. Chen, S. Parker, MPDI Plasma **1** 105 (2018)

[Idomura05] Y. Idomura et al, Nucl. Fusion **45** 1571 (2005)

[Jenko00] F. Jenko et al., Phys. Plasmas **7** 1904 (2000)

[Jenko04] F. Jenko, Plasma Fusion Res. **11** 11 (2004)

[Kuley15] A. Kuley, et al., Phys. Plasmas **22** 102515 (2015)

[Kenser99] J. Kesner and S. Migliuolo, Nucl. Fusion **39** 163 (1999)

[YLin05] Y. Lin, X. Wang, Z. Lin and L. Chen, Plasma Phys. Contr. Fus. **47** 657 (2005)

[Langer82] W.D. Langer, Nuc. Fusion **22** 751 (1982)

[Lin05] Z. Lin, L. Chen, F. Zonca, Phys. Plasmas **12** 56125 (2005)

[Lin07] Z. Lin, et al., Phys. Rev. Lett. **99** 265003 (2007)

[Maeyama15] S. Maeyama et al., Phys. Rev. Lett. **114** 255002 (2015)

[Manz14] P. Manz, et al., Plasma Phys. Controlled Fusion **56** 035010 (2014)

[Miecniowski18] M. Miecniowski, B. Sturdevant, Y. Chen, S. Parker, Phys. Plasmas **25** 055901 (2018).

[Mitchell19] M. S. Mitchell, M. T. Miecniowski, G. Beylkin, and S. E. Parker, J. Comput. Phys. **396** 837 (2019)

[Miller 98] R. Miller, M. Chu, J. Greene, Y. Lin-Liu, R. Waltz, Phys. Plasmas **5** 973 (1998)

[Mishchenko14] A. Mishchenko, et al., Phys. Plasmas **21** 092110 (2014)

[Moradi13] S. Moradi, et al., Nucl. Fusion **53** 063025 (2013)

[Nevins05] W.M. Nevins et al., Phys. Plasmas **12** 122305 (2005)

[Nevins07] W.M. Nevins, et al., Physics of Plasmas **14** 084501 (2007)

[Numata11] R. Numata, et al., Phys. Plasmas **18** 112106 (2011)

[Parker06] S.E. Parker, et al. AIP Conf. Proc. **871** 193 (2006)

[Predebon10] I. Predebon, et al., Phys. Rev. Lett. **105** 195001 (2010)

[Predebon13] I. Predebon and F. Sattin, Phys. Plasmas **20** 040701 (2013)

[Roach05] C. Roach, et al., Plasma Phys. Contr. Fusion **47** B323 (2005)

[Rogers07] B. Rogers, et al., Phys. Plasmas **14** 092110 (2007)

[Rosenbluth98] M. Rosenbluth, F. Hinton, Phys. Rev. Lett. **80** 724 (1998)

[Saarelma13] S. Saarelma, et al., Nucl. Fusion **53** 123012 (2013)

[Similon84] P.L. Similon, P.H. Diamond, Phys. Fluids **27** 916 (1984)

[Schnack13] D. Schnack, J. Cheng, D. Barnes, S. Parker, Phys. Plasmas **20** 063106 (2013)

[Smith11] D. Smith, et al., Plasma Phys. Controlled Fusion **53** 035013 (2011)

[Spong12] D. Spong, et al., Phys. Plasmas **19** 082511 (2012)

[Srivastav19] P. Srivastav et al., Plasma Phys. Control. Fusion **61** 055010 (2019)

[Startsev14] E. Startsev, W. Lee, Phys. Plasmas **21** 022505 (2014)

[Sturdevant16] B. Sturdevant, S. Parker, Y. Chen, B. Hause, J. Comput. Phys. **316** 519 (2016)

- [Sturdevant17] B. J. Sturdevant, Y. Chen, S. E. Parker, Phys. Plasmas **24** 081207 (2017)
- [Sydora01] R. Sydora, Phys. Plasmas **8** 1929 (2001)
- [Tanaka1993] M. Tanaka, J. Comp. Phys. **107** 124 (1993)
- [Terry83] P.W. Terry, W. Horton, Phys. Fluids **26** 106 (1983)
- [Todo10] Y. Todo, H. L. Berk, and B. N. Breizman, Nucl. Fusion **50** 084016 (2010)
- [Told08] D. Told, et al., Phys. Plasmas **15** 102306 (2008)
- [Wakatani84] M. Wakatani, A. Hasegawa, Phys. Fluids **27** 611 (1984)
- [Wan05] W. Wan, Y. Chen and S. Parker, Phys. Plasmas **12** 012311 (2005)
- [Wan10] W. Wan, S. E. Parker, Y. Chen, F.W. Perkins, Phys. Plasmas **17**, 040701 (2010)
- [Wan11] W. Wan, S. E. Parker, et al., Phys. Plasmas **18**, 056116 (2011)
- [Wan15] W. Wan, et al., Phys. Plasmas **22** 062502 (2015)
- [Wan17] B.N. Wan et al., Nucl. Fusion **57** 102019 (2017)
- [Wang12] E. Wang, et al., Nucl. Fusion **52**, 103015 (2012)
- [Wang18] F. Wang, et al., Plasma Phys. Control. Fusion **60** 125005 (2018)
- [Wesson11] “Tokamaks,” 4th edition, J. Wesson, Oxford Science Publications (2011)
- [Wong07] K. Wong, et al., Phys. Rev. Lett. **99** 135003 (2007)
- [Yamoto17] S. Yamoto, et al., Nucl. Fusion **57** 116051 (2017)
- [Yu15] P. Yu et al., Comput. Phys. Comm. **192** 32 (2015)